

Superconducting Phase Domains for Memory Applications

S. V. Bakurskiy,^{1,2,3} N. V. Klenov,^{1,2,3} I. I. Soloviev,^{1,3} M. Yu. Kupriyanov,^{1,3} and A. A. Golubov^{3,4}

¹*Skobeltsyn Institute of Nuclear Physics, Lomonosov Moscow State University, Leninskie gory, Moscow 119991, Russian Federation*

²*Faculty of Physics, Lomonosov Moscow State University, Leninskie gory, Moscow 119992, Russian Federation*

³*Moscow Institute of Physics and Technology, Dolgoprudny, Moscow Region, 141700, Russian Federation*

⁴*Faculty of Science and Technology and MESA+ Institute for Nanotechnology, University of Twente, 7500 AE Enschede, The Netherlands*

(Dated: April 9, 2018)

In this work we study theoretically the properties of S-F/N-sIS type Josephson junctions in the frame of the quasiclassical Usadel formalism. The structure consists of two superconducting electrodes (S), a tunnel barrier (I), a combined normal metal/ferromagnet (N/F) interlayer and a thin superconducting film (s). We demonstrate the breakdown of a spatial uniformity of the superconducting order in the s-film and its decomposition into domains with a phase shift π . The effect is sensitive to the thickness of the s layer and the widths of the F and N films in the direction along the sIS interface. We predict the existence of a regime where the structure has two energy minima and can be switched between them by an electric current injected laterally into the structure. The state of the system can be non-destructively read by an electric current flowing across the junction.

PACS numbers: 74.45.+c, 74.50.+r, 74.78.Fk, 85.25.Cp

Josephson junctions containing normal (N) and ferromagnetic (F) materials in a weak link region are currently the subject of intense research. An interest in such structures is due to the possibility of their use as control elements of superconductor memory compatible with Single Flux Quantum (SFQ) logic. A number of implementations of Josephson control elements were proposed recently, among which the structures containing F layers in the weak link region are of greatest interest¹⁻³. Various types of superconducting spin-valve structures including two or more ferromagnetic layers have been proposed⁴⁻¹⁸. The mutual orientations, parallel or antiparallel, of magnetizations of the layers determine critical currents and critical temperatures of the structures. Recently, it was proposed to apply the phenomenon of triplet superconductivity in spin-valve devices with noncollinear magnetization of the layers¹⁹⁻²⁷. The problem of small characteristic voltage $I_C R_N$ in these structures was solved by using an additional tunnel barrier connected through a thin superconducting spacer²⁸⁻³¹. However, to control an operation of these devices, the application of magnetic fields or strong spin-polarized currents is necessary in order to switch the structure to a different state. Such control requires the use of additional external circuits resulting in restriction of possible memory density. Moreover, characteristic operational times of such devices are limited by relatively slow processes of the remagnetization of the ferromagnetic layers.

In this work we propose a S-N/F-s-I-S control unit for a superconducting memory cell (Fig.1) based on the principles completely different as the suggested earlier. The considered structure consists of the two superconductive electrodes (S) and of the two weak link regions: the tunnel barrier (I) and the metallic (N/F) interlayer. The (N/F) part is formed by the longitudinally oriented normal (N) and ferromagnetic (F) layers. The weak link areas are separated by a thin superconducting s-layer (see Fig.1). We consider the phenomenon of nucleation of the Superconducting Phase Domains (SPD) in the thin s-layer induced by proximity effect with the bulk superconducting S-electrode through the complex ferromagnetic

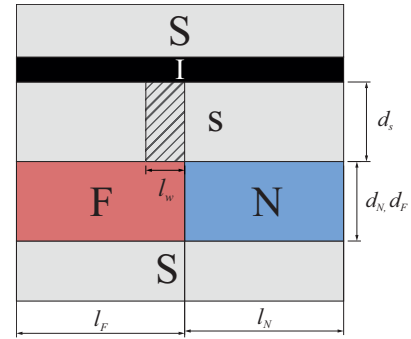


FIG. 1: The sketch of S-N/F-s-I-S structure. Thickness of the superconducting, ferromagnetic and normal metal films are denoted as d_s , d_N and d_F , respectively. The longitudinal lengths of ferromagnetic and normal metal films are denoted as l_F and l_N . A probable area of SPD-wall formation is hatched in the figure and determined by the length l_w .

interlayer. We propose the way to control a switching between the SPD-state and the single domain state of the junction. To provide the quantitative model of the structure, we solve self-consistently the two-dimensional boundary-value problem in the frame of the quasiclassical Usadel equations in the diffusive regime³²⁻³⁶.

Superconducting Phase Domains. Let's consider the S-N/F-s-I-S structure shown in Fig.1. We suppose that dirty limit conditions are fulfilled for all metals and use the Usadel equations³² with Kupriyanov-Lukichev³⁶ boundary conditions at the interfaces. To simplify the calculations, we also assume that all metals have equal resistivities $\rho_F = \rho_N = \rho_S$ and the coherence lengths $\xi_F = \xi_N = \xi_S = \sqrt{D_{S,N,F}/\pi T_C}$, while the ferromagnetic material is characterized by the exchange energy H . In addition, we neglect suppression of superconductivity in the S electrodes due to the inverse proximity effect, while the superconducting properties of the middle s-layer are found in a self-consistent manner. Finally, we assume that all spatial dimensions of the structure are much smaller than the Josephson penetration depth λ_J and there are

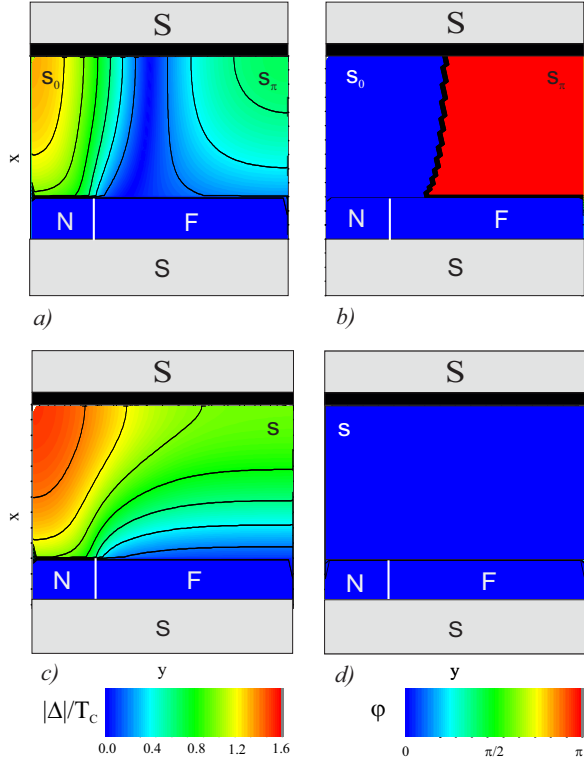


FIG. 2: The distribution of the magnitude (a, c) and the phase (b, d) of the pair potential Δ over the S-F/N-s-I-S structure for various thicknesses of s-layer: (a, b) for $d_s = 3.5\xi_S$ and (c, d) for $d_s = 4\xi_S$. Thinner superconducting layers are separated into two domains of 0 and π phases, while thicker films stay in the single domain state with the 0 phase. The chosen parameters of the structure are: $d_F = 1\xi_F$, $l_F = 12\xi_S$, $l_N = 4\xi_S$, the exchange energy $H = 10\pi T_C$ and the suppression parameter³⁶ $\gamma_B = 0.3$.

no vortices inside the structure.

The state of the S-N/F-s-I-S structure significantly depends on thickness of the intermediate s-layer. In Fig.2 the results of numerical calculations of the pair potential in the intermediate N/F-s layer are demonstrated for different thicknesses of the s-layer. On the bottom panels (c) and (d) the spatial distributions of the pair potential in the relatively thick s-film with $d_s = 4\xi_S$ are shown. The calculations demonstrate that only the magnitude of the s-film order parameter varies in space, while there is no spatial variation of its phase ϕ . This state is defined as the 0-state of the junction.

For thinner s-film with $d_s = 3.5\xi_S$, two superconducting domains separated by the area of suppressed superconductivity are clearly distinguished (Fig.2a, b). The superconducting phase ϕ varies between these domains: $\phi = 0$ in the domain in the vicinity of the N-layer and $\phi = \pi$ in the vicinity of the F-layer. We call this state as the Superconducting Phase Domain State (SPD-state) and define the domains as s_0 and s_π , respectively.

The nature of this phenomenon can be understood in terms of the SFs and SNs junctions connected in parallel. It is well known that the π -state might be realized in the SFs part of the structure³⁷. In the case of a thick s-layer, we deal with the 0- π junction with the SFs and SNs channels connected in parallel. Such configurations have been discussed earlier in re-

lation to possible realization of ϕ -junctions³⁸⁻⁴². The ground state phase ϕ of the junction depends on the relation between the Josephson energies of the SFs and the SNs parts

$$E_{JF} = \frac{\hbar j_{CF} l_F W}{2e}, \quad E_{JN} = \frac{\hbar j_{CN} l_N W}{2e}, \quad (1)$$

where $j_{CF,N}$ are the critical current densities of the SFs and SNs junctions, respectively, and $l_{F,N}W$ are their cross-section areas. Since the energy of the SNs-junction is typically larger than that of the SFs one, the SNs-junction controls the phase $\phi = 0$ of the s-layer. As long as we consider the regime when the SFs-junction is in a π -state, the phase $\phi = 0$ is energetically unfavorable for the SFs part of the device.

The situation may drastically change with the decrease of the s-layer thickness. As will be shown below, at a certain critical thickness the s-film splits into two separate superconducting domains with phases shifted by π .

To perform simple estimates of the critical s-layer thickness and the thickness of the domain wall, one should compare the energies of SFs junction E_{JF} and of the domain wall E_{SPD} . The latter has two contributions

$$E_{SPD} = E_w + 2E_{Jw} = \Delta F_w l_w d_s W + \frac{\hbar j_{Cw} d_s W}{e}. \quad (2)$$

The first one, E_w , is the superconducting condensation energy of the volume with suppressed superconductivity. This term is proportional to the volume of the domain wall and increases linearly with the growth of its thickness l_w . The second term E_{Jw} is the Josephson coupling energy of the junction between 0 and π domains. This term decreases with the growth of l_w due to the suppression of the Josephson current density $j_{Cw} \sim \text{Exp}(-l_w)$. Minimizing the $E_{SPD}(l_w)$ functional, one can estimate the width l_w , which is of the order of ξ_S , in agreement with the results of the numerical calculations (Fig.2a). Further, using the condition of SPD-state formation

$$E_w + 2E_{Jw} \leq 2E_{JF} \quad (3)$$

and taking the typical junction parameters from Fig.2, one can estimate characteristic value of the critical s-layer thickness, which is of the order of few ξ_S .

One has to take into account that in same range of s-layer thicknesses superconductivity in the s-layer might be suppressed due to an inverse proximity effect^{29,30}. However, since the critical thickness d_s of the SPD-state formation is proportional to the lateral size l_F , the latter can be chosen large enough to tune d_s to larger values and thus to avoid suppression of superconductivity. Numerical calculations show that $l_F = 12\xi_F$ is sufficient to observe the SPD state.

Further, we note that since the lateral size of the junction is smaller than λ_J , one can neglect magnetic fields generated by currents in the structure and therefore disregard half-quantum vortices which might be trapped in the junction and destroy the SPD state.

Control unit for memory element. In this section we discuss possible application of the S-N/F-s-I-S device as a control unit for a memory element. While the thickness of the

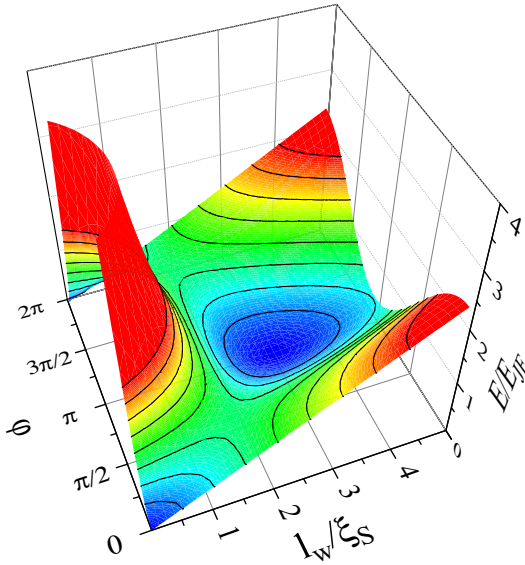


FIG. 3: Energy profile in the S-F/N-s-I-S structure versus phase φ of the s_π domain and thickness of the domain wall l_w . The parameters of the SPD-state $E_{Jw} = 0.25E_{JF}$ and $E_w = 1.5E_{JF}$ are chosen so that system is in the critical regime between the 0 and SPD-states. In this case, the double-well potential forms two local minima: the minimum in the left corner corresponds to the 0-state and the one in the middle corresponds to SPD-state.

intermediate s -layer d_s is close to the critical one, the S-F/N-s-I-S system stays in the vicinity of the transition between 0- and SPD-states.

To model the system, we take into account the Josephson energies of the junctions and the pairing energy of s -layer and we treat the domain wall as a normal layer with finite thickness l_w . The energy of the system depends on the thickness l_w and on the phase φ of the s_π domain, neglecting small Josephson energy of the sIS junction:

$$E = E_{JF}(1 - \cos(\pi - \varphi)) + E_w + E_{Jw}(1 - \cos \varphi) - 2E_{JF}. \quad (4)$$

Fig. 3 shows the energy profile of the system in the regime when the thickness d_s is close to its critical value calculated from Eqs.(2,4). It is seen that there are two local minima at the phases $\varphi = 0$ and $\varphi = \pi$, which correspond to the 0- and SPD- states. The 0-state local minimum is obtained at $l_w = 0$ and corresponds to the absence of the region of suppressed superconductivity. Contrary, the SPD- state is realized at a finite thickness l_w . These states are separated by a potential barrier, which provides the possibility to store an information.

"Write" and "Read" operations. Below we propose how to perform "Write" and "Read" operations in the considered device in the regime with two local energy minima existing simultaneously (Fig. 3). When an injected current is extracted through the right arm of the structure (Fig. 4a,b), the junction switches into the SPD-state. Alternatively, for the left-side current extraction (Fig. 4c,d), the junction switches into the 0-state.

To illustrate the operation principle, we start from the 0-state (Fig. 4a). Since the current phase relation of the SFs junction has an additional π -shift, total Josephson current is the superposition of two opposite supercurrents across the

SNs and SFs parts of the junction. In the competing SPD-state (Fig.4b) the total critical current is larger than in the 0-state since the backflow through the SFs junction is limited by the domain wall. As a result, switching from 0-state into the energetically more favorable SPD-state should occur with an increase of the external current, as illustrated in Fig.4e. When the current is switched off the junction remains in the SPD-state.

In the case when the current is extracted from the left side, the distribution of currents in the SPD-state significantly change (Fig. 4d), and the junction behaves as a π -junction with additional backflow through the N-layer. In the competing 0-state Fig. 4c, the junction has higher value of the critical current and lower energy. Therefore, switching from the SPD-

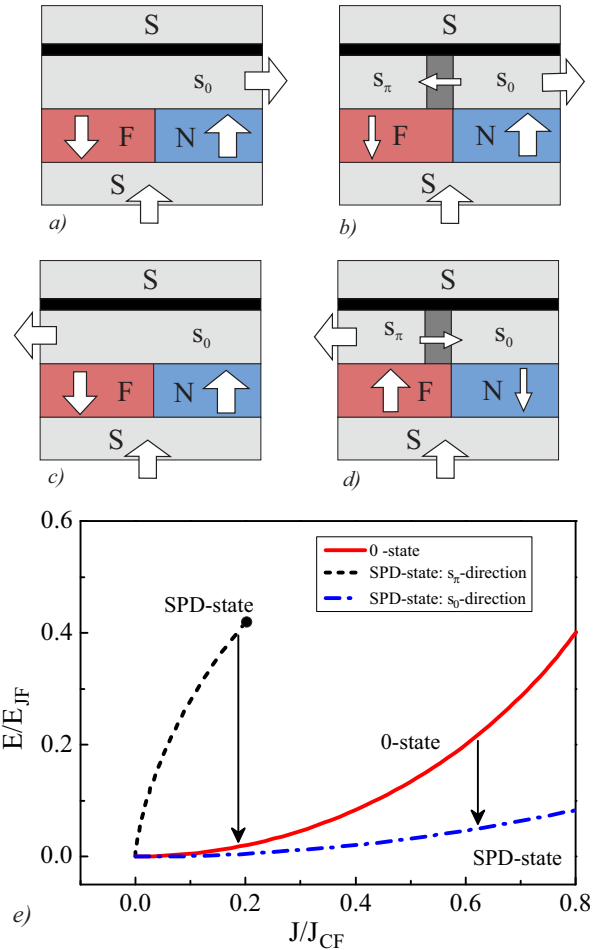


FIG. 4: Schematic current distribution over the structure for the "Write" operation in the 0-state (a,c) and the SPD-state (b,d). The chosen parameters are $E_{Jw} = 0.8E_{JF}$, $E_{JN} = 4E_{JF}$ and $E_w = 0.4E_{JF}$. The arrows demonstrate the directions in which the current flows. e) Energies of the SPD and 0- states versus current for different connections of electrodes. Current J is normalized on the critical current of the SFs part of the junction J_{CF} . The solid line corresponds to the 0-state (independent from type of connection), the dashed line corresponds to the SPD state with electrode connected to s_π region, and dash-dotted line corresponds to the SPD- state with the electrode connected to the s_0 domain.

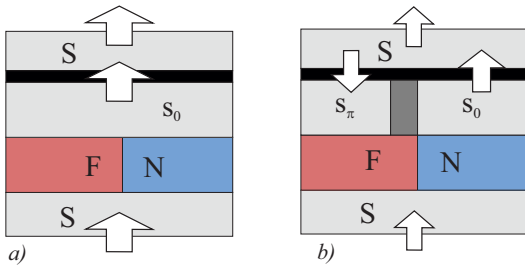


FIG. 5: Schematic current distribution across the structure for the "Read" operation in the 0-state (a) and the SPD-state (b). The arrows demonstrate directions in which the current flows. In the 0-state the current is homogeneously distributed over the tunnel barrier, while in the SPD-state the current is separated over two channels with opposite directions of flow. Hence, the latter state has the smaller critical current.

state into the more favorable 0-state should occur (see Fig.4e).

A "Read" operation can be implemented by a vertical current flowing across the whole structure (Fig. 5). In this case, the weak link of the Josephson junction is located at the tunnel barrier I and the critical current is much smaller than in the previously discussed cases. Hence, this current can not change the state of the junction and the magnitude of the critical current is determined only by the superconducting order parameters in the vicinity of the tunnel barrier. In the 0-state, the current is distributed homogeneously over the whole tunnel barrier, while in the SPD-state, there are separated domains in the s-layer with a phase difference π and the current through the tunnel barrier consists of two channels with opposite current directions. The total current in the latter state is much smaller than in the former. Therefore, the system can

be used as a control unit for a memory element.

Discussion. The performed analysis of the Josephson effect in SIs(F/N)S structures suggests the possibility for the existence of superconducting phase domains in the s-layer.

This phenomenon is not only of fundamental interest, but can also be used for the realization of a control unit for superconducting memory cells. The proposed unit has several noticeable advantages in comparison with the existing solutions.

First, for its operation it is enough to have only one ferromagnetic film in the weak link region. This opens the way for the realization of a control unit with a large $I_C R_N$ product close to that for tunnel junctions used in RSFQ logical circuits.

Second, switching between the equilibrium states doesn't require remagnetization of the ferromagnetic layers, i.e. application of a strong external magnetic field or spin-polarized currents. All "write" and "read" operations are implemented by Josephson currents and never deal with time scales specific to remagnetization processes. The characteristic time of the considered device is based on mechanisms of destruction and recovery of superconductivity in the thin s-film. This time is determined by properties of electron-phonon interaction in the superconductor. These processes are similar to those in superconducting single photon detectors⁴³ and can have a timescale in the order of 100 – 1000 ps depending on material constants of the s-layer.

Thus, the phenomenon of superconducting phase domains looks promising for memory applications.

Acknowledgment. This work was supported by the Russian Science Foundation, Project No. 15-12-30030.

- ¹ M.G. Blamire, J.W.A. Robinson, *Journal of Physics Condensed Matter*, **26**, 453201 (2014).
- ² M. Eschrig, *Reports on Progress in Physics*, **78**, 104501 (2015).
- ³ J. Linder, J. W. A. Robinson, *Nature Physics*, **11**, 307 (2015).
- ⁴ J. Y. Gu, C.-Y. You, J. S. Jiang, J. Pearson, Ya. B. Bazaliy, and S. D. Bader, *Phys. Rev. Lett.*, **89**, 267001 (2002).
- ⁵ C. Bell, G. Burnell, C. W. Leung, E. J. Tarte, D.-J. Kang and M. G. Blamire, *Appl. Phys. Lett.*, **84**, 1153 (2004).
- ⁶ S. Oh, D. Youm, and M. Beasley, *Appl. Phys. Lett.* **71**, 2376 (1997).
- ⁷ M. A. E. Qader, R. K. Singh, Sarah N. Galvin, L. Yu, J. M. Rowell, and N. Newman, *Appl. Phys. Lett.*, **104**, 022602 (2014).
- ⁸ B. Baek, W.H. Rippard, S.P. Benz, S.E. Russek, and P.D. Dresselhaus, *Nature Communications*, **5**, 3888 (2014).
- ⁹ J. W. A. Robinson, N. Banerjee, and M. G. Blamire, *Phys. Rev. B* **89**, 104505 (2014).
- ¹⁰ B. M. Niedzielski, S. G. Diesch, E. C. Gingrich, Y. Wang, R. Loloee, W. P. Pratt, Jr., and N. O. Birge, *IEEE Trans. Appl. Supercond.*, **24**, 1800307 (2014).
- ¹¹ B. Li, N. Roschewsky, B. A. Assaf, M. Eich, M. Epstein-Martin, D. Heiman, M. Munzenberg, and J. S. Moodera, *Phys. Rev. Lett.* **110**, 097001 (2013).
- ¹² Yuanzhou Gu, Gabor B. Halasz, J.W.A. Robinson, and M.G. Blamire, *Phys. Rev. Lett.* **115**, 067201 (2015).
- ¹³ V. I. Zdravkov, J. Kehrle, G. Obermeier, D. Lenk, H.-A. K. von Nidda, C. Muller, M. Y. Kupriyanov, A. S. Sidorenko, S. Horn, R. Tidecks, L. R. Tagirov, *Phys. Rev. B* 2013, **87**, 144507 (2013).
- ¹⁴ P. V. Leksin, N. N. Garif'yanov, I. A. Garifullin, Ya. V. Fominov, J. Schumann, Y. Krupskaya, V. Kataev, O. G. Schmidt, and B. Buchner, *Phys. Rev. Lett.* **109**, 057005 (2012).
- ¹⁵ Y. V. Fominov, A. A. Golubov, T. Yu. Karminskaya, M. Yu. Kupriyanov, R. G. Deminov, L. R. Tagirov, *JETP Lett.* 2010, **91**, 308.
- ¹⁶ A. Iovan, T. Golod, and V. M. Krasnov, *Phys. Rev. B*, **90**, 134514 (2014).
- ¹⁷ M. Alidoust, and K. Halterman, *Phys. Rev. B* **89**, 195111 (2014).
- ¹⁸ L. R. Tagirov, *Phys. Rev. Lett.* **83**, 2058 (1999).
- ¹⁹ N. Banerjee, J.W.A. Robinson, M.G. Blamire, *Nature Communications* **5**, 4771 (2014).
- ²⁰ M. Houzet and A. I. Buzdin, *Phys. Rev. B* **76**, 060504(R) (2007).
- ²¹ F. S. Bergeret, A. F. Volkov, and K. B. Efetov, *Phys. Rev. Lett.* **86**, 3140 (2001).
- ²² T. S. Khaire, M. A. Khasawneh, W. P. Pratt, and N. O. Birge, *Phys. Rev. Lett.* **104**, 137002 (2010).
- ²³ M. S. Anwar, M. Veldhorst, A. Brinkman, and J. Aarts, *Appl. Phys. Lett.* **100**, 052602 (2012).
- ²⁴ C. Klose, T. S. Khaire, Y. Wang, W. P. Pratt, Jr., N. O. Birge, B. J. McMorran, T. P. Ginley, J. A. Borchers, B. J. Kirby, B. B. Maranville, and J. Unguris, *Phys. Rev. Lett.* **108**, 127002 (2012).
- ²⁵ T. Yu. Karminskaya, M. Yu. Kupriyanov, and A. A. Golubov, *Pis'ma v ZhETF* **87**, 657 (2008) [*JETP Lett.* **87**, 570 (2008)].
- ²⁶ G. B. Halasz, M. G. Blamire, and J. W. A. Robinson, *Phys. Rev.*

- B 84**, 024517 (2011).
- ²⁷ M. Alidoust, J. Linder, Phys. Rev. B, **82**, 224504 (2010).
- ²⁸ T. I. Larkin, V. V. Bol'ginov, V. S. Stolyarov, V. V. Ryazanov, I. V. Vernik, S. K. Tolpygo, and O. A. Mukhanov, Appl. Phys. Lett. **100**, 222601 (2012).
- ²⁹ S. V. Bakurskiy, N. V. Klenov, I. I. Soloviev, V. V. Bol'ginov, V. V. Ryazanov, I. I. Vernik, O. A. Mukhanov, M. Yu. Kupriyanov, and A. A. Golubov, Appl. Phys. Lett. **102**, 192603 (2013).
- ³⁰ S. V. Bakurskiy, N. V. Klenov, I. I. Soloviev, M. Yu. Kupriyanov, A. A. Golubov, Phys. Rev. B **88**, 144519 (2013).
- ³¹ N. Ruppelt, H. Sickinger, R. Menditto, E. Goldobin, D. Koelle, R. Kleiner, O. Vavra, H. Kohlstedt, Appl. Phys. Lett., **106**, 022602 (2015).
- ³² K. D. Usadel, Phys. Rev. Lett. **25**, 507 (1970).
- ³³ A. A. Golubov, M. Yu. Kupriyanov, E. Il'ichev, Rev. Mod. Phys. **76**, 411 (2004).
- ³⁴ A. I. Buzdin, Rev. Mod. Phys. **77**, 935 (2005).
- ³⁵ F. S. Bergeret, A. F. Volkov, K. B. Efetov, Rev. Mod. Phys. **77**, 1321 (2005).
- ³⁶ M. Yu. Kupriyanov and V. F. Lukichev, Zh. Eksp. Teor. Fiz. **94**, 139 (1988) [Sov. Phys. JETP **67**, 1163 (1988)].
- ³⁷ V.V. Ryazanov, V.A. Oboznov, A.Yu. Rusanov, A.V. Veretennikov, A.A. Golubov, J. Aarts, Phys. Rev. Lett. **86**, 2427 (2001).
- ³⁸ A. Buzdin and A. E. Koshelev, Phys. Rev. B **67**, 220504(R) (2003).
- ³⁹ E. Goldobin, D. Koelle, R. Kleiner, and R.G. Mints, Phys. Rev. Lett. **107**, 227001 (2011).
- ⁴⁰ S. V. Bakurskiy, N. V. Klenov, T. Yu. Karminskaya, M. Yu. Kupriyanov, and A. A. Golubov, Supercond. Sci. Technol. **26**, 015005 (2013).
- ⁴¹ H. Sickinger, A. Lipman, M. Weides, R. G. Mints, H. Kohlstedt, D. Koelle, R. Kleiner, E. Goldobin, Phys. Rev. Lett. **109**, 107002 (2012).
- ⁴² I. I. Soloviev, N. V. Klenov, S. V. Bakurskiy, V. V. Bol'ginov, V. V. Ryazanov, M. Yu. Kupriyanov, A. A. Golubov, Appl. Phys. Lett., **105**, 242601 (2014).
- ⁴³ G. N. Gol'tsman, O. Okunev, G. Chulkova, A. Lipatov, A. Semenov, K. Smirnov, B. Voronov, A. Dzardanov, C. Williams, R. Sobolewski, Appl. Phys. Lett. **79**, 705 (2001).